European Water 58: 53-60, 2017.

Bimetal doping on TiO_2 for photocatalytic water treatment: A green route

V. Rao Chelli and A.K. Golder*
Department of Chemical Engineering, Indian Institute of Technology Guwahati, Assam, Pin 781039, India
* *e-mail: animes@iitg.ernet.in*

Abstract: Herein, we propose a new and green technique of bio-mediated bimetal doping on TiO_2 ($Zn/Cu/TiO_2$) using the aqueous leaf extract of Chayote plant which is rich in ascorbic acid (354 mg/kg leafs). The proposed method was successful to bring down the band gap of TiO_2 to 2.3 eV for $Zn/Cu/TiO_2$ at 1:1:98. The crystallite size of TiO_2 at higher dopants loading was increased significantly (16.3 to 38.4 nm) because of Cu^{2+} and Zn^{2+} induction into the Ti^{4+} lattice and, there was as high as 12% transformation of the anatase phase to the rutile phase of TiO_2. The increase in the absolute value of zeta-potentials of $Cu/Zn/TiO_2$ was notably faster (5 mV per unit pH increase) at $pH>pH_{zpc}$ which was resulted from the rise in oxygen vacancies and, $Cu/Zn/TiO_2$ were mostly present as a separated non-aggregated unit in water with a polydispersity index of 0.201. $Zn/Cu/TiO_2$ exhibited 98% Congo red dye decolourization compared to 59.3 and 68.7% with Zn/TiO_2 and Cu/TiO_2 under the visible light illumination (17700 Lux). COD reduction was 80.6, 71.2, and 75.9% with $Zn/Cu/TiO_2$, Zn/TiO_2, and Cu/TiO_2 with the quantum efficiency of 23.4, 30.8 and 41.5%, respectively. It was found that $O_2^{\bullet-}$ radicals were mostly caused the dye decomposition as evidenced from the electron spin resonance spectroscopy.

Key words: Bimetal doped photocatalyst; Band gap reduction; Visible light absorption; Dye degradation

1. INTRODUCTION

The heterogeneous photocatalysis using TiO_2 is one of the most preferred advanced oxidation processes for the treatment of such effluents (Riaz et al., 2013). The catalyst is easily available, cheap, non-toxic and enough chemical stability (Behera et al., 2016). However, bare TiO_2 is only active in UV region. Therefore, to make it active in the visible region, doping with the transition metals is a common technique (Riaz et al., 2013).

Bi-metal doped photocatalyst shows a better photocatalytic activity than the mono-metal doping or bare systems in many times (Malika et al., 2016; Riaz et al., 2013; Tobaldi et al., 2016). The doping techniques and dopant metal composition could considerably differ the activity of photocatalysts (Malika et al., 2016). Ag and Au doped TiO_2 shows around 3-fold rise in the phenol decomposition rate for bi-metal doped photocatalyst compared to mono-metal doping [8]. Cu and Zn bimetal-doped TiO_2 synthesized by sol–gel method increases the visible light aided photocatalytic activity by a factor 1.5-2 times compared to pristine TiO_2 for decomposition of methyl orange dye (Zhang and Zeng, 2011). Tobaldi et al. synthesized $Cu/Ni/TiO_2$ photocatalyst by thermal induced sol-gel process and reported bi-metal doped TiO_2 is more effective than and mono-metal doping in degradation of gas-solid phase nitrous oxides and isopropanol than decolorization of orange II (Tobaldi et al., 2016).

The visible light absorption could enhance with bi-metal doping and stimulate faster photo-generated electron (e^-) transfer to dopant metal from TiO_2 owing to increase the separation of e^- and hole (h^+) (Malika et al., 2016). The recombination of e^-/h^+ and its separation, plays a key role on the photocatalytic activity. Cu and Zn are low-cost and easily available than many transition metals.

The conventional techniques for metals doping on semiconductor supports are employed by hazardous chemical intensive (Harraz et al., 2013), high thermal energy intensive (Wen et al., 2007) and UV photo-reduction (Bokare et al., 2013). The preferred size and morphology can be attained by these techniques but they are expensive, complex as well as harmful for the environment.

Here we use a bio-inspired method of metal doping on the semiconductor supports mediated by

plant extract as the reserve of the analytes (reducing agent). This work focus on Cu/Zn bimetal-doping on TiO_2 support using the analytes such ascorbic acid (Chelli and Golder, 2016; Ordonez et al., 2006; Rao and Golder, 2016) present in *S. edule* leaf-extract. Thus, the aim of this study was the bio-mediated doping of Cu and Zn on TiO_2 in a bimetallic system for the determination of its impact on dye degradation efficiency. The photocatalysts were characterized in terms of XRD patterns, DR-UV–vis spectroscopy, FTIR spectroscopy and zeta-potentials. The catalytic activity of Cu/TiO_2, Zn/TiO_2, and $Cu/Zn/TiO_2$ was studied for degradation of Congo red (CR) dye and determination of quantum yield (QY).

2. MATERIALS AND METHODS

2.1 Reagents

Deionized water (dH_2O) was prepared using Millipore water synthesis system (Elix-3, USA) for reagent and dye solution preparations. $Zn(NO_3)_2{,}6H_2O$ (99% w/w purity), $CuSO_4.5H_2O$ (99% w/w purity), $K_2Cr_2O_7$ (99.9% purities w/w), $AgSO_4$ (98.5% purities w/w), $HgSO_4$ (99% purities w/w), NaOH (98% w/w purity), H_2SO_4 (98% v/v purity), and KBr (99.5% w/w purity) were obtained from Merck, Mumbai. TiO_2 (99% w/w purity) containing 80% anatase and 20% rutile by weight was procured from Sigma Aldrich, India. Congo Red (CR) dye (696.6 g/mol, 96% w/w purity) was supplied by Loba Chemie, Mumbai. All chemicals were used as received without further purification.

2.2 Preparation of bio-extract extract

Fresh 20 g *Sechium edule* leaves were collected from the nearby locality, and were washed with dH_2O. They were shredded into small pieces, 100ml dH_2O was added and the mixture was stirred for 30 minutes at 80 ºC. Then the solution was filtered and chayote leaves extract was collected in an amber glass container and stored at 4 ºC for further use.

2.3 Bio-mediated doping method

Metal precursors $CuSO_4$ and $ZnNO_3$ were used respectively to prepare Cu and Zn mono and bi-metal nanoparticles. TiO_2 powder (2 g) was added in 200 mL of $CuSO_4$ solution corresponding to Cu-concentration 2 g per 100 g catalyst. The obtained mixture was stirred for 60 min to facilitate adsorption of Cu^{2+} on TiO_2. Then it was centrifuged at 4000 rpm for 30 min, and the supernatant was analysed for the residual Cu^{2+} concentration. The Cu^{2+}/TiO_2 residue was further dispersed in 180 mL dH_2O, and a 20 mL *S. edule* extract was added with stirring at 300 rpm on a magnetic stirrer for 24 h. The brown colour Cu doped TiO_2 (Cu/TiO_2) residue was filtered out and rinsed 4 times with ethanol and dH_2O. Cu/TiO_2 was dried at 100 ^oC in a hot-air oven (N-101, Navyug, India) for 12 h and ground in a mortar and pestle. The synthesized Cu/TiO_2 particles were stored in an airtight container in dark. Similar procedure was employed for the preparation of Zn/TiO_2 (2:98% w/w) as well as bimetal doped $Cu/Zn/TiO_2$ (1:1:98% w/w).

2.4 Analytical techniques

FTIR spectra were recorded within the wavenumber ranging from 400 to 4000 cm^{-1} (IR affinity-1, Shimadzu, Japan). KBr was first dried for 2 h at 110 °C to remove water and mixed with the sample at 99:1 ratio before pelletization. The diffuse reflectance of synthesized photocatalyst was acquired in the range of 250 to 1200 nm using UV-vis Spectroscopy of Shimadzu, Japan (Solid

Spec 3700/3700DUV). The X-ray diffraction (XRD) (model: D8 11 Adavnce, bruker, Germany) pattern were obtained at 2 angle from 20 to 80º with a step of 0.05º and integration time of 0.5 s. Zeta-potential was measured at different pH solution (Delsa nano analyser, Beckman Coulter, Switzerland). pH measurement was performed using a precision pH meter of Eutech Instruments (pH/ion 510, Malaysia). The dye concentration was monitored by UV-vis Spectroscopy (UV 2300, M/s Thermo Fisher India).

2.5 Photocatalytic activity test using bio-mediated Cu/Zn-doped TiO_2

Photocatalytic degradation of 100 ppm CR dye was conducted with visible light irradiation at different initial pH (3-11). The catalyst was added to the solution and then the suspension was stirred in dark for 30 minutes to equilibrate on the catalyst surface before illumination. A visible lamp of 200 W/250 V (17 K Lux, M/s Bajaj Electricals Ltd., India) was then irradiated for 2 h at different catalyst loadings with continuous stirring. The collected samples were analysed for residual dye concentration by using UV-vis spectrophotometer.

3. RESULTS AND DISCUSSION

3.1 Determination of Cu and Zn loading onto TiO_2

Cu^{2+} and Zn^{2+} uptake efficieny of TiO_2 with the equilibrium (after 1 h of adsorption) Cu^{2+} and Zn^{2+} concentration is illustrated in Table 1. The initial concentration of Cu^{2+} and Zn^{2+} was maintained 2 % (w/w) each and for bimetal 1:1 % (w/w) per 10 g TiO_2. The time of doping test was set to 24 h. It was selected from a trial run of only Cu^{2+} and Zn^{2+} precursor and bio-extract without TiO_2 and, the formation of Cu and Zn-nanoparticle were complete in 24 h. The efficiency of Cu and Zn-doping was found to be 80.7 and 74.2% with 2% (w/w) each which were obtained in the pre-immobilization (adsorption) study. It implies that the true loading of Cu and Zn onto TiO_2 was about 1.61 and 1.48 (w/w w.r.t. Cu/TiO_2 and Zn/TiO_2). There was insignificant amount of Cu^{2+} and Zn^{2+} ions leached out in the solution during the doping test.

Ascorbic acid (AA) was found to be the most abundant compound (176.92 m/z) (Rao and Golder, 2016) in *S. edule* which was consisting of 354 mg AA/kg leafs. AA is an ideal e^- donor which can reduce metal ions into zero valence leading to nucleation onto the TiO_2.

Table 1. Quantitative retention of Cu^{2+} and Zn^{2+} ions onto TiO_2.

Catalyst	Ionic matter	Initial loading, % (w/w)	True loading, % (w/w) on TiO_2	% Residual concentration	
				After 1 h adsorption	After 48 h reaction
Cu/TiO_2	Cu^{2+}	2	1.614	19.3	1.43
Zn/TiO_2	Zn^{2+}	2	1.484	25.8	1.76
$Cu/Zn/TiO_2$	Cu^{2+}	1	0.938	6.2	0.5
	Zn^{2+}	1	0.792	20.8	0.9

3.2 Characteristics of $Cu/Zn/TiO_2$

3.2.1 X-ray diffractogram

The XRD patterns of pristine, mono- and bi-metal doped $Cu/Zn/TiO_2$ are shown in Figure 1. It exhibited the major characteristic peaks of highly crystalline TiO_2. The intense peaks at $2\theta = 25.34$, 37.85 and 48.15º confirm the crystalline planes of anatase phase. Whereas $2\theta = 27.45$, 35.98, 41.42 and 54.21º attribute to the rutile phase. Three additional characteristic peaks appeared at 41.8, 50.1

and 73.9º were corresponding to the (1 1 1), (2 0 0) and (2 2 0) crystalline planes of face-centered cubic structured Cu nanoparticles (JCPDS No. 04-0836, a = 3.609 Å) and, a small peak observed at 61.1º associated to (2 2 0) plane of Cu_2O (Cuya Huaman et al., 2011). Similarly two more peaks at 31.6 and 67.9º corresponding to (1 0 0) and (1 1 2) planes of ZnO nanoparticles (JCPDS No. 361451) (Bala et al., 2015). The existence of Cu/Zn species also conformed by the EDX image mapping (Figure 2). It displays that assembles of numerous nanoparticles by the structural functionalization comprising of Ti, O, Cu and Zn elements. The crystallite size was determined by using the Scherrer's equation (Rao and Golder, 2016). The crystallite size for the intense peak of anatase phase at (1 1 1) plane was found to be 16.66, 22.38, 38.2 and 24.84 nm nm for TiO_2, Cu/TiO_2, Zn/TiO_2, $Cu/Zn/TiO_2$, respectively. The same for the rutile phase at (1 1 0) plane was calculated as 28.21, 29.46, 32.75 and 65.68 nm, respectively. The change in the size of crystal lattice is dependent with the variation in the ionic radius of the metal dopants (Malika et al., 2016). The induction of larger ionic radius metal dopants into the Ti^{4+} lattice was resulted in higher crystallite size. The anatase phase was found as 80.06, 81.38, 70.47 and 76.54% for TiO_2, Cu/TiO_2, Zn/TiO_2, $Cu/Zn/TiO_2$, respectively, from the integrated peak intensities at (1 0 1) and (1 1 0) planes (Rao and Golder, 2016). It indicates a maximum of 12% phase transmission from anatase to rutile. A similar trend of crystallite size increment was reported by Behnajady and Eskandarloo (Behnajady and Eskandarloo, 2013) in the case of bi-metal doped TiO_2.

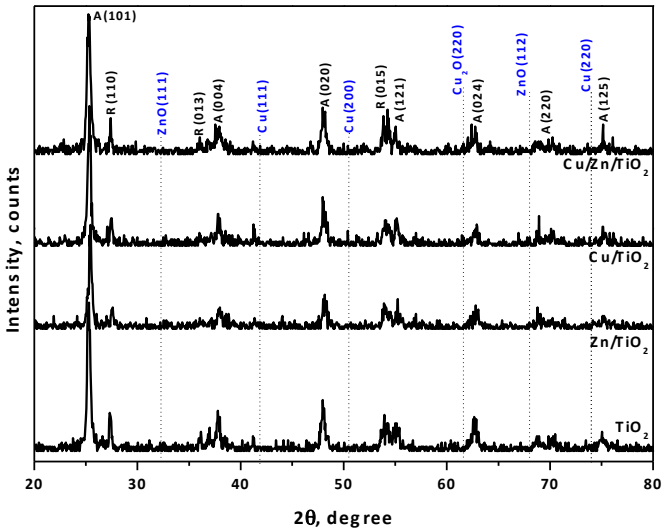

Figure 1. XRD patterns of bare, mono and Cu/Zn bimetal doped TiO_2 nanostructures.

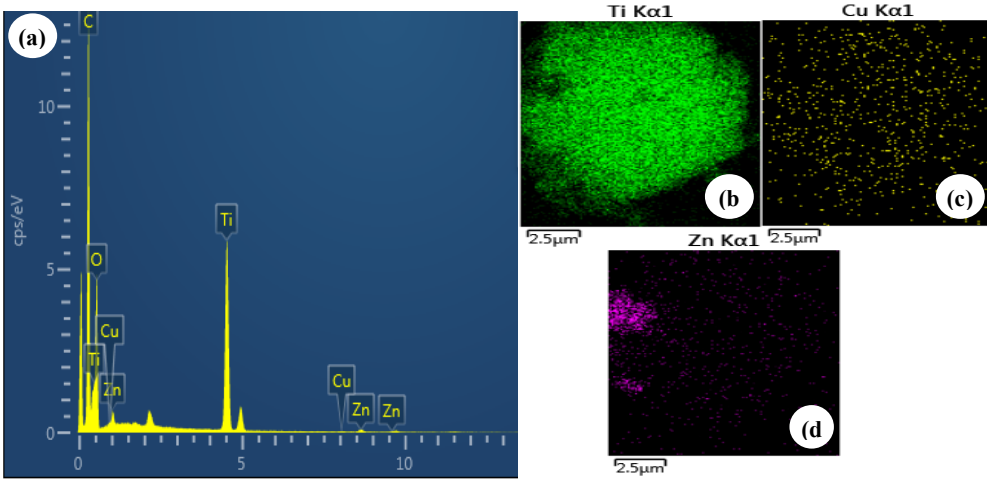

Figure 2. (a): Relative dispersity of Ti, O, Cu and Zn elements, (b-d): Dispersity of individual element Ti, Cu and Zn.

3.2.2 Spectral absorbance of bio-mediated doped Cu/Ni/TiO_2

An intense absorption peak in the UV domain (Figure 3) can be noticed for pristine TiO_2, which is assigned to the band-to-band transition (Malika et al., 2016). A maximum absorption band around 315 nm in the TiO_2 spectrum related to the route of charge transferring from O^{2-} (2p) to Ti^{4+} (3d) (Paulino et al., 2016). Cu doping displayed an important absorption tail in the visible domain from 400 to 800 nm. The band at 250–310 nm is assigned to the ligand-to-dopant charge transfer formation of Cu^{2+}(3d) from O^{2-}(2p), happening in separated Cu^{2+} locates. In addition, the band at 340 nm is evidence that the existence as well as large distribution of $(Cu–O–Cu)^{2+}$ assembles. In the case of Zn-doping, the energy absorption spectrum poses a maximum wavelength near to 400 nm little above to TiO_2. Cu/Zn/TiO_2 absorption spectrum exhibited a broader band than the other photocatalysts spectra, indicating greater photocatalytic activity.

The band gap energy (E) of doped catalysts was determined using the indirect transition model also called Touc plot (Rao and Golder, 2016) (Figure 3 (Inset)). TiO_2 showed E of 3.05 eV whereas Zn doping (2%, w/w) alone did not reduce much. However, Cu-doping showed a superior performance in band gap reduction with 2.397 eV. The change in E suggests that the induction of Cu changes the material functionalization, owing a reallocation of its electrical charge. Cu acts as a h^+ scavenger leading to a lengthier isolation between the e^-/h^+ pairs produced by enhancing material photoefficiency. As it was expected, Zn-doping did not stimulate a reduction in E for Cu/Ni/TiO_2 since its E value (2.79 eV) is small raise to that of TiO_2. Paulino et al. also reported the band gap results of 3.17, 2.95 and 3.02 eV with TiO_2, Cu/TiO_2, Cu/Zn/TiO_2, respectively (Paulino et al., 2016).

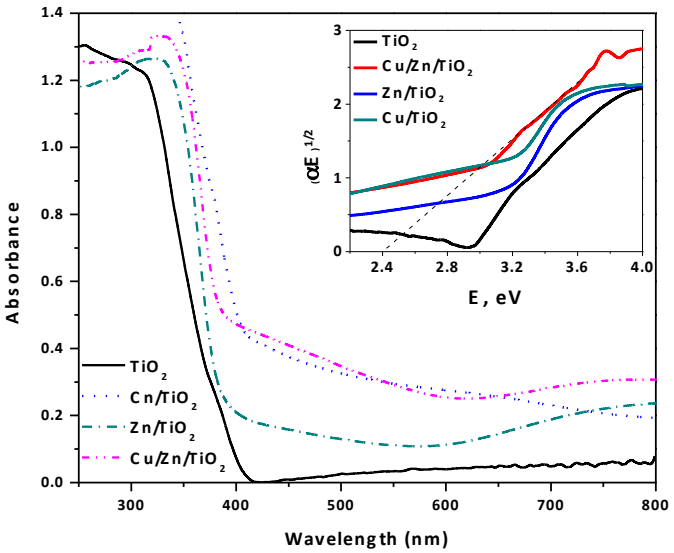

Figure 3. UV–vis DR spectra of pristine, mono and bimetal-doped TiO_2. Inset: Optical direct band gaps (Tauc plot).

3.2.3 FTIR spectra of Cu/Zn/TiO_2

FTIR spectra of pristine, mono and bimetal doped TiO_2 particles are shown in Figure 4(a). The bands at 3460 and 1600 cm^{-1} attributed to the OH–stretching and OH–bending modes, respectively of physically absorbed moisture. A small band observed at 2891 cm^{-1} can be assigned to dimer –OH (Behera et al., 2016). The metal-doped TiO_2 enhanced the surface adsorption of –OH and water groups. Ti^{4+} in TiO_2 lattice substituted by Cu^{2+} and Zn^{2+} ions and formed Cu–O or Zn–O. It enhances the oxygen vacancies that are equilibrated by the adsorption of more H_2O or –OH groups (Malika et al., 2016). The peaks detected at 472, 523, and 482 cm^{-1} are for the stretching mode of Ti–O, Cu–O, and Zn–O, respectively (Malika et al., 2016; Tobaldi et al., 2016). A wide peak observed at 1184 cm^{-1} can be attributed to scissoring mode of H_2O molecule. A band at 783 cm^{-1}

corresponding to Ti-O was shifted to 727 and 732 cm^{-1} after doping because of Cu–O–Ti and Zn–O–Ti stretching asymmetric vibrations. These changes were detected due to the defects raised by the induction of metal dopants into TiO_2 lattice (Behera et al., 2016).

3.2.4 Colloidal stability of TiO_2 and Cu/Zn/TiO_2

The polydispersity index was found to be 0.201 for Cu/Zn/TiO_2 which is a measure of the size distribution of particles in an aqueous colloidal sample. The zeta-potentials (ξ) of bare TiO_2 and doped Cu-Zn/TiO_2 are presented in Figure 4(b). ξ were measured for different pH (from 3 to 10) to understand the behaviour of surface charge of modified TiO_2 in its aqueous solution. The zero point charge (pH_{zpc}) was dropped from 6.42 to 5.91 after doping of TiO_2. The pH_{zpc} is potentially affect the adsorption behaviour of organic compounds on the photocatalyst surface during a photocatalytic reaction (Malika et al., 2016). The surface of the photocatalyst is positively charged below pH_{zpc} and carries a negative charge above it. A low pH_{zpc} indicates a higher concentration of OH^- ions on the surface of catalyst. The raise in the induced oxygen vacancies enhances the surface adsorbed –OH groups that leads to an increase in the surface charge due to the metal doping (Rao and Golder, 2016). At higher pH, more negative charged particles were observed due to higher electrostatic repulsion which prevents the formation of agglomerates as well as enhances the colloidal stability with raise in ξ towards more negative (Behera et al., 2016). It shows that Cu-Zn/TiO_2 particles are comparatively greater stable at higher pH.

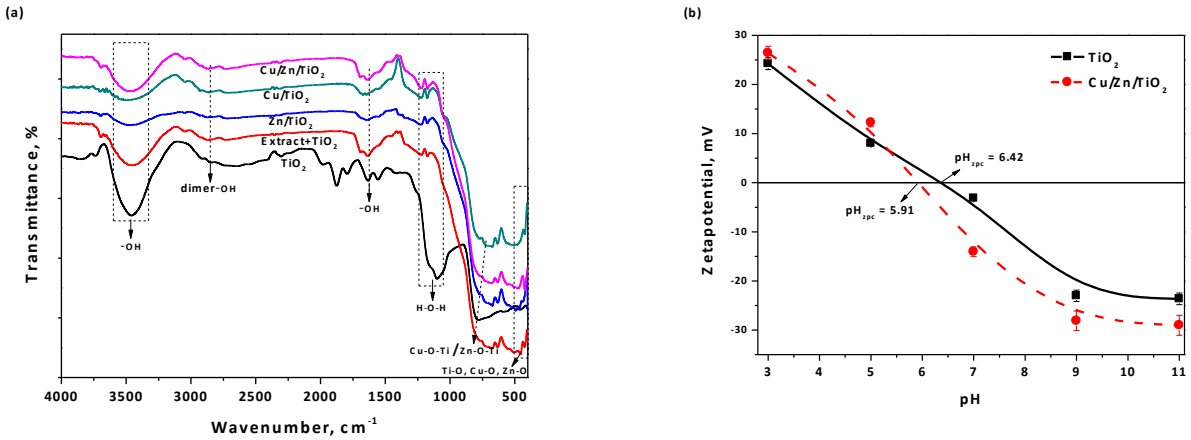

Figure 4. (a) FTIR Spectra for different catalysts (b) Effect of pH on the zeta-potential for bare and doped TiO_2.

3.3 Cu/Zn/TiO_2 photocatalytic performance under visible light

It was found that there was about 98% CR decomposition at pH 5 with Cu/Zn/TiO_2 upto irradiation time of 120 min (Figure 5). It was 14.1, 68.7 and 59.3 % in the case of TiO_2, Cu/TiO_2 and Zn/TiO_2 with the similar experimental condition which is line with the optical response of photocatalysts in the visible region (Figure 3). The results indicate that the bimetal doped TiO_2 was more efficient than mono-metal doping under the visible light irradiation. The activity of Cu/TiO_2 was also better than Zn/TiO_2 indicating that the Cu doping could enhance the charge separation effectively with a low recombination rate.

It was observed that bi-metal doped catalyst showed the maximum COD (chemical oxygen demand) removal of 80.6% as compared to mono-metal doped as well as bare TiO_2 (Figure 5). The COD removal was found to be 10.5, 75.9 and 71.2% for TiO_2, Cu/TiO_2 and Zn/TiO_2, respectively, which is following the similar trend of CR dye colour removal.

The quantum yield (QY) for the degradation of CR dye was also determined (Shidpour, 2015) (Figure 5). The maximum QY was found to be 41.5% in 120 min of reaction time for Cu/Ni/TiO_2.

The QY of bio-mediated Cu/Zn-doped TiO_2 was more than many earlier reports (Kusiak-Nejman et al., 2011; Li et al., 2012). The $O_2^{\bullet-}$ radicals were mostly responsible for the degradation of CR dye as evidenced from the electron spin resonance spectra (results not shown here).

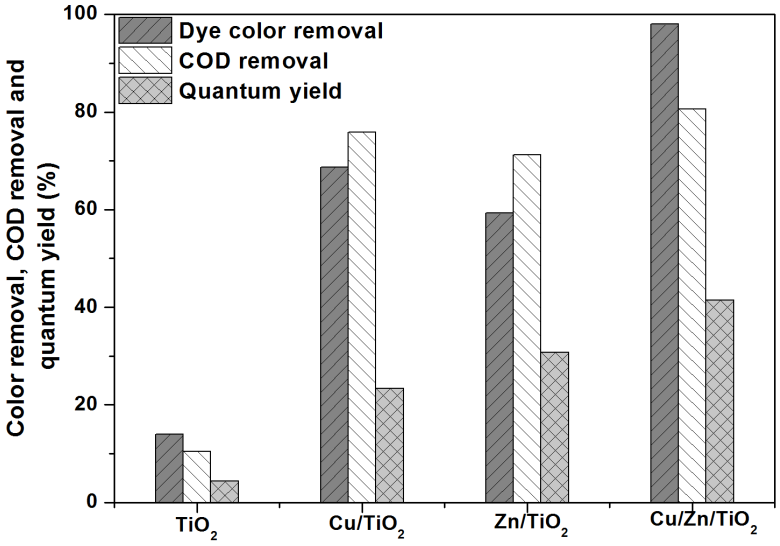

Figure 5. Congo red dye color, COD removal, and quantum yield for bare and doped catalysts.

4. CONCLUSIONS

The bio-mediated co-metal doping of Cu and Zn onto TiO_2 showed a significant decrease in the band gap energy than the mono-metal doping at the same weight loading. This technique increased the crystallite size in bimetal doping for both anatase and rutile phases. The absolute zeta potential value was more with bimetal doping which is indicative of a better tendency to oppose the destabilization. The visible light aided degradation of CR dye with Cu/Zn/TiO_2 was significantly higher, and could cause almost complete decolourization in 2 h. The quantum yield of bimetal doped TiO_2 catalyst in the current study exhibited a clear superiority over many existing studies using conventional doping methods.

REFERENCES

Bala, N., Saha, S., Chakraborty, M., Maiti, M., Das, S., Basu, R., Nandy, P., 2015. Green synthesis of zinc oxide nanoparticles using Hibiscus subdariffa leaf extract: effect of temperature on synthesis, anti-bacterial activity and anti-diabetic activity. RSC Adv. 5, 4993–5003. doi:10.1039/C4RA12784F

Behera, A.K., Rao, C.V., Das, R.K., Giri, A.S., Golder, A.K., 2016. Fabrication and characterization of Ag-doped titania: impact of dye-sensitization, phenol decomposition kinetics and biodegradability index. Desalin. Water Treat. 57, 9488–9497.

Behnajady, M.A., Eskandarloo, H., 2013. Silver and copper co-impregnated onto TiO2-P25 nanoparticles and its photocatalytic activity. Chem. Eng. J. 228, 1207–1213.

Bokare, A., Pai, M., Athawale, A.A., 2013. Surface modified Nd doped TiO2 nanoparticles as photocatalysts in UV and solar light irradiation. Sol. Energy 91, 111–119.

Chelli, V.R., Golder, A.K., 2016. pH dependent size control, formation mechanism and antimicrobial functionality of bio-inspired AgNPs. RSC Adv. 6, 95483–95493. doi:10.1039/C6RA16475G

Cuya Huaman, J.L., Sato, K., Kurita, S., Matsumoto, T., Jeyadevan, B., 2011. Copper nanoparticles synthesized by hydroxyl ion assisted alcohol reduction for conducting ink. J. Mater. Chem. 21, 7062–7069. doi:10.1039/c0jm04470a

Harraz, F.A., Abdel-Salam, O.E., Mostafa, A.A., Mohamed, R.M., Hanafy, M., 2013. Rapid synthesis of titania-silica nanoparticles photocatalyst by a modified sol-gel method for cyanide degradation and heavy metals removal. J. Alloys Compd. 551, 1–7.

Kusiak-Nejman, E., Janus, M., Grzmil, B., Morawski, A.W., 2011. Methylene Blue decomposition under visible light irradiation in the presence of carbon-modified TiO2 photocatalysts. J. Photochem. Photobiol. A Chem. 226, 68–72. doi:10.1016/j.jphotochem.2011.10.018

Li, B., Liu, T., Wang, Y., Wang, Z., 2012. ZnO/graphene-oxide nanocomposite with remarkably enhanced visible-light-driven photocatalytic performance. J. Colloid Interface Sci. 377, 114–121. doi:10.1016/j.jcis.2012.03.060

Malika, M., Rao, C.V., Das, R.K., Giri, A.S., Golder, A.K., 2016. Evaluation of bimetal doped TiO2 in dye fragmentation and its comparison to mono-metal doped and bare catalysts. Appl. Surf. Sci. 368, 316–324.

Ordonez, A.A.L., Gomez, J.D., Vattuone, M.A., Isla, M.I., 2006. Antioxidant activities of Sechium edule (Jacq.) Swartz extracts. Food Chem. 97, 452–458. doi:10.1016/j.foodchem.2005.05.024

Paulino, P.N., Salim, V.M.M., Resende, N.S., 2016. Zn-Cu promoted TiO2 photocatalyst for CO2 reduction with H2O under UV light. Appl. Catal. B Environ. 185, 362–370. doi:10.1016/j.apcatb.2015.12.037

Rao, C.V., Golder, A.K., 2016. Development of a bio-mediated technique of silver-doping on titania. Colloids Surfaces A Physicochem. Eng. Asp. 506, 557–565.

Riaz, N., Chong, F.K., Man, Z.B., Khan, M.S., Dutta, B.K., 2013. Photodegradation of Orange II under visible light using Cu–Ni/TiO_2: Effect of calcination temperature. Ind. Eng. Chem. Res. 52, 4491–4503.

Shidpour, R., 2015. A Power-law relationship between characteristics of light source and quantum yield in photocatalytic systems. J. Phys. Chem. C 119, 22425–22431. doi:10.1021/acs.jpcc.5b02318

Tobaldi, D.M., Piccirillo, C., Rozman, N., Pullar, R.C., Seabra, M.P., Skapin, A.S., Castro, P.M.L., Labrincha, J.A., 2016. Effects of Cu, Zn and Cu-Zn addition on the microstructure and antibacterial and photocatalytic functional properties of Cu-Zn modified TiO_2 nano-heterostructures. J. Photochem. Photobiol. A Chem. 330, 44–54. doi:10.1016/j.jphotochem.2016.07.016

Wen, Z., Wang, G., Lu, W., Wang, Q., Zhang, Q., Li, J., 2007. Enhanced photocatalytic properties of mesoporous SnO2 induced by low concentration ZnO doping. Cryst. Growth Des. 7, 1722–1725.

Zhang, D., Zeng, F., 2011. Photocatalytic oxidation of organic dyes with nanostructured zinc dioxide modified with silver metals. Russ. J. Phys. Chem. A 85, 1077–1083. doi:10.1134/S0036024411080073.